Published in final edited form as:
Eur J Med Chem. 2021 April 05; 215: 113257. doi:10.1016/j.ejmech.2021.113257.

Faropenem reacts with serine and metallo-β-lactamases to give multiple products

Anka Lucic[#a], **Philip Hinchliffe**[#b], **Tika R. Malla**[#a], **Catherine L. Tooke**[b], **Jürgen Brem**[a], **Karina Calvopiña**[a], **Christopher T. Lohans**[c], **Patrick Rabe**[a], **Michael A. McDonough**[a], **Timothy Armistead**[b], **Allen M. Orville**[d], **James Spencer**[b,+], **Christopher J. Schofield**[a,+]

Christopher T. Lohans: christopher.lohans@queensu.ca; Allen M. Orville: allen.orville@diamond.ac.uk

[a]Chemistry Research Laboratory, The Department of Chemistry and the Ineos Oxford Institute for Antimicrobial Research, 12 Mansfield Road, Oxford OX1 3TA, United Kingdom

[b]Cellular and Molecular Medicine, Biomedical Sciences Building, University Walk, Bristol, BS8 1TD, United Kingdom

[c]Botterell Hall, Kingston, Ontario, Canada, K7L 2V7

[d]Diamond House, Harwell Science and Innovation Campus, Didcot, OX11 0DE

[#] These authors contributed equally to this work.

Abstract

Penems have demonstrated potential as antibacterials and β-lactamase inhibitors; however, their clinical use has been limited, especially in comparison with the structurally related carbapenems. Faropenem is an orally active antibiotic with a C2 tetrahydrofuran (THF) ring, which is resistant to hydrolysis by some β-lactamases. We report studies on the reactions of faropenem with carbapenem-hydrolysing β-lactamases, focusing on the class A serine β-lactamase KPC-2 and the metallo β-lactamases (MBLs) VIM-2 (a subclass B1 MBL) and L1 (a B3 MBL). Kinetic studies show that faropenem is a substrate for all three β-lactamases, though it is less efficiently hydrolysed by KPC-2. Crystallographic analyses on faropenem-derived complexes reveal the opening of the β-lactam ring with formation of an imine with KPC-2, VIM-2, and L1. In the cases of the KPC-2 and VIM-2 structures, the THF ring is opened to give an alkene, but with L1 the THF ring remains intact. Solution state studies, employing NMR, were performed on L1, KPC-2, VIM-2, VIM-1, NDM-1, OXA-23, OXA-10, and OXA-48. The solution results reveal, in all cases, formation of imine products in which the THF ring is opened; formation of a THF ring-closed imine product was only observed with VIM-1 and VIM-2. An enamine product with a closed THF ring was also observed in all cases, at varying levels. Combined with previous reports, the results exemplify the potential for different outcomes in the reactions of penems with MBLs and SBLs

[+]Correspondence to be sent to these authors. christopher.schofield@chem.ox.ac.uk, jim.spencer@bristol.ac.uk.

Author Contributions

A.L., P.H. and C.L.T. crystallised proteins and solved and refined the X-ray data with help from M.A.M and J.B. T.R.M measured the NMR data and analysed with help from C.T.L. A.L., P.H., C.L.T, P.R., K.C and C.T.L produced enzymes. P.H., C.L.T and T.A. collected kinetic data. A.L., P.H., T.R.M., and C.J.S. drafted the manuscript. P.H., J.S. and C.J.S. designed and conceived the research. All authors edited the manuscript.

Conflicts of Interest

The authors declare no competing financial interests.

Europe PMC Funders Author Manuscripts

and imply further structure-activity relationship studies are worthwhile to optimise the interactions of penems with β-lactamases. They also exemplify how crystal structures of β-lactamase substrate/inhibitor complexes do not always reflect reaction outcomes in solution.

Keywords

antimicrobial resistance; β-lactams; penems; carbapenems; β-lactams; serine-β-lactamases; metallo-β-lactamases

1.0 Introduction

β-Lactams are presently the most prescribed antibacterials, though their efficacy is being eroded by antimicrobial resistance[1]. The best characterised of such mechanisms involves β-lactamase-catalysed hydrolysis (Figure 1). β-Lactamases of Ambler classes A, C and D[2] are nucleophilic serine enzymes (serine β-lactamases, SBLs). Class B comprises of zinc-dependent metallo-β-lactamases (MBLs)[3,4], which are divided into sub classes B1, B2 and B3, based on sequence, structure and zinc ion utilisation. The B1 and B3 MBLs employ two zinc ions, whereas the B2 MBLs employ a single zinc ion[5].

Clinically-available carbapenems are synthetic antibiotics that are used intravenously to treat serious bacterial infections[7]. Although once considered last-resort drugs, in part because of their inhibition of some SBLs, extensive carbapenem use has resulted in the dissemination of carbapenem-hydrolysing β-lactamases, such as the class A SBL *Klebsiella pneumoniae* carbapenemase-2 (KPC-2), which is now present in multiple Gram-negative pathogens, including *Klebsiella pneumoniae*, *Escherichia coli* and *Acinetobacter spp.*[8,9]. Some class D SBLs (including OXA-48, OXA-23 and OXA-10[10]) can also manifest carbapenemase activity. The role of MBLs in carbapenem resistance is growing; indeed, B1 (e.g. VIM and NDM MBLs) and B3 (e.g. L1) MBLs can efficiently hydrolyse almost all β-lactam antibiotics, excluding monobactams (Figure 1)[3,11].

One factor in determining the β-lactamase susceptibility of β-lactam substrates and inhibitors is the stability of the complexes formed between the enzyme and the substrate / inhibitor. The ability of carbapenems to form relatively stable complexes with both their antibacterial transpeptidase targets and SBLs is an important factor in their efficacy relative to other β-lactams[12]. However, the precise factors that determine the stability of such complexes are incompletely understood, as exemplified by a recent report that carbapenems can react with class D SBLs to produce β-lactones as well as hydrolysed products (Figure 2)[10,13]. Studies on the products of carbapenem hydrolysis by representative MBLs and SBLs suggest that the initial hydrolysis products are predominantly in the enamine tautomeric form, and can undergo subsequent non-enzymatic tautomerisation to the more stable imine isomer[10,14].

Studies on carbapenems[11,12] led us to investigate the hydrolysis mechanism of penems[15] by selected SBLs and MBLs. Penems are closely related to the carbapenems by structure but contain a thiazoline rather than a pyrroline ring (Figure 1). The penems were developed in the 1970s in attempts to combine the structures of the penicillins and

Europe PMC Funders Author Manuscripts

cephalosporins to give more stable and efficacious drugs[16]; they have a broad spectrum of activity against both Gram negative and Gram positive bacteria[17] although they have little efficacy against *Pseudomonas aeruginosa*[18]. Penems also have the potential to act as potent SBL inhibitors, as exemplified by BRL 42715[19], which potently inhibits SBLs, including those from the OXA, SHV and TEM subfamilies[20]. BRL 42715 reacts with the nucleophilic serine to form an acyl-enzyme complex which subsequently rearranges to form a cyclic amino-acrylate derivative (Figure S1)[19].

Faropenem is an orally active penem antibiotic with a tetrahydrofuran (THF) C-2 side chain; it is used extensively in Asia to treat respiratory and urinary tract infections[21,22]. Faropenem is currently the only penem in clinical use, with sulopenem presently in clinical trials[23]. Like the carbapenems, faropenem inhibits some SBLs, including the class C enzyme AmpC and extended spectrum SBLs such as BlaC and members of the CTX-M family[24,25]. Faropenem is, however, susceptible to hydrolysis by carbapenemases such as the B1 MBLs, e.g. NDM-1. There are reported crystal structures of complexes formed by the reaction of faropenem with transpeptidases (PBP3 and LdtMt2)[26,27] and SBLs (KPC-2, BlaC, OXA-48 and SED-G238C)[28], though these crystal structures were not correlated with the reaction products in solution (Figure 3).

Here we report studies using steady-state kinetics, X-ray crystallography, and NMR on the reaction of faropenem with SBLs and MBLs. We initially focused on the class A SBL KPC-2 and the class B1 and B3 MBLs VIM-2 and L1. VIM-2 is a widely disseminated, clinically important, broad spectrum B1 MBL[29]. The B3 MBL L1 is a broad spectrum MBL, chromosomally encoded by *Stenotrophomonas maltophilia* and which has the same overall fold as class B1 MBLs, though it differs in its Zn2 ion coordination[30]. The combined production of L1 and a class A SBL (L2) makes infections by *S. maltophilia* difficult to treat. Crystallographic analyses of faropenem-derived complexes suggest that with KPC-2 and VIM-2, the THF ring opens to give an alkene product, but with L1 the ring remains intact. Subsequent NMR solution studies on the faropenem derived reaction products with multiple β-lactamases reveal the formation of both imine and enamine products The THF ring was observed in both the opened and closed forms, with the precise product profiles being enzyme specific. Note in contrast to crystallographic findings, the THF ring intact hydrolysis product was not observed for L1.

2 Results

2.1 Faropenem hydrolysis by β-lactamases in solution

We initially determined steady state kinetic parameters for faropenem hydrolysis by the carbapenemases KPC-2, VIM-2, and L1 by monitoring the hydrolysis of the faropenem β-lactam ring at λ 306 nm (with 10 nM enzyme) (Table 1). Comparison of turnover numbers (k_{cat}) reveals that, under saturating conditions, VIM-2 and L1 hydrolyse faropenem at a rate ~10 times greater than KPC-2, though the L1 K_M is higher than that for KPC-2 or VIM-2. The catalytic efficiency (k_{cat}/K_M) of KPC-2 with faropenem is ~5- and 33-fold lower than for L1 or VIM-2, respectively. We also observed weak substrate (faropenem) inhibition of KPC-2 (K_i ~44 μM).

2.2 Crystallographic determination of faropenem products

We next sought to investigate how the faropenem-derived products interact with the active sites of VIM-2, KPC-2, and L1. To obtain a crystal structure of the faropenem derived complex with KPC-2, we substituted Glu166, which is important for deacylation of the acyl-enzyme intermediate (Figure 1), for the isosteric Gln (KPC-2^{E166Q}) that prevents antibiotic turnover[33]. Pre-formed KPC-2^{E166Q}, VIM-2, and L1 crystals were then soaked with a faropenem solution (see methods for details) to obtain X-ray diffraction datasets with resolutions extending to 1.25 Å, 1.29 Å and 1.57 Å, respectively (Table S1). VIM-2 crystallised in two different space groups, $I22$ and $C2$ [32,33] with one or two protein molecules in the asymmetric unit, respectively. KPC-2 and L1 crystallised in space groups $P2_12_12$[34] and $P6_422$[35], both with one molecule in the asymmetric unit (Figure S2). In all four datasets, electron density in the active site is consistent with the presence of a faropenem-derived product with an opened β-lactam ring (Figure 4).

2.2.1 KPC-2 Structure—With KPC-2, the faropenem-derived species is covalently bound to Ser70; the C2 atom is sp^2 hybridized and its THF ring is opened to give an imine alkene product (Figures 4D and S3). The exocyclic C-2 – C-11 alkene (Figure S3 and Figure S4A) is present as the Z-isomer, a feature that could not be resolved in our NMR studies (see below). An analogous complex was also observed with VIM-2 (see below). Electron density for THF-derived atoms is more poorly defined than for the rest of the ligand in both KPC-2 and VIM-2, manifesting as higher B-factors, likely due to a lack of defined interactions with protein (Figure S4B-D). A prior crystallographic study of KPC-2 with faropenem resulted in the observation of a non-covalently bound hydrolysed product at the active site, which was modelled and refined as the enamine form with the THF ring intact[36] (Figure 3); however, electron density is notably absent for the entire THF side chain, so the exact nature of the ligand is uncertain.

The β-lactam derived carbonyl oxygen is positioned in the oxyanion hole, forming hydrogen bonds with the backbone amides of Ser70 and Thr237, consistent with observations for acyl-enzyme complexes of other SBLs (Figure 4D and Figure S3A)[6]. Additional polar interactions include the C-10 carboxylate with Thr235 and the C-6 hydroxyethyl oxygen with Asn132. A hydrophobic interaction of the fragmented THF ring is made with Trp105 (Figure S3B), a residue involved in interactions with substrates and SBL inhibitors, e.g. relebactam [34]. The interactions of hydrolysed faropenem with KPC-2 resemble those of meropenem with SFC-1 (PDB 4EV4[37]), a class A SBL that, like KPC-2, can hydrolyse carbapenems (Figure S5). Notably, the hydroxyethyl chain is orientated away from the deacylating water in both the KPC-2: faropenem and SFC-1: meropenem-derived structures, being positioned to form a hydrogen bond with Asn132. This orientation is suggested to be favourable for hydrolysis, whereas in carbapenem-inhibited class A enzymes, the deacylating water is thought to be deactivated by interaction with the hydroxyethyl group[37].

In our KPC-2: faropenem complex, there is a conformational change in the catalytically important Ω-loop, relative to its location in the unreacted enzyme (Figure S6). This results in two conformations of Gln166, (which is the general base for the deacylation step [38]).

In one conformation Gln166 is directed into the active site in a manner that enables it to interact with the deacylating water; in the other conformation, it is directed out of the active site (Figure S6). We have previously observed a similar movement of Glu166 in molecular dynamics simulations of KPC-2 with hydrolysed ceftazidime in the active site, which we attributed as the major factor for the poor turnover of ceftazidime by KPC-2 [33]. Therefore, this conformational dynamic may also contribute to the relatively slow turnover rate for KPC-2 with faropenem (Table S1).

2.2.2 VIM-2 Structure—Interactions of the faropenem-derived hydrolysis product with VIM-2 are equivalent in both the *I*222 (soaking time: 30 mins) and *C*2 (soaking time: 5 hours) structures (Figure 4A, 4B and Figure S7; standard MBL numbering is used throughout[39]). As with KPC-2, faropenem reacts with VIM-2 to give an imine-alkene, as crystallographically observed (Figure 1). One of the oxygen molecules of the newly formed C-7 carboxylate displaces the Zn-bridging water molecule (Figures 4 and 5). This results in an increase in the Zn1-Zn2 distance (4.2 Å) compared to the un-complexed VIM-2 (PDB 4BZ3, 3.5 Å), as has been observed on the binding of some MBL inhibitors, e.g. bicyclic boronates, to VIM-2 (Figure S8)[39]. The C-7 carboxylate hydrogen bonds with the Asn233 sidechain amide group (Figure 5) and the C-6 hydroxyethyl oxygen hydrogen bonds with the Asp120 backbone amide. Binding is further stabilised by hydrophobic interactions between faropenem-derived elements and Phe61 and Tyr67 on loop L3 (a region of the active site often involved in interactions with substrates and inhibitors[40–42]) and Trp87 in the active site (Figure S7B and S7C).

2.2.3 L1 Structure—Crystallographic analysis reveals that the reaction of faropenem with L1 results in an imine with the THF ring remaining closed; this occurs *via* protonation at C-2, which is clearly defined by the electron density as being sp^3 hybridized and in the (*S*)-configuration (Figure 4C and Figure S9). The C-7 carboxylate and C-6 hydroxyethyl sidechain are rotated in comparison with the orientations observed in the KPC-2 and VIM-2 faropenem complexes (Figure S10). Furthermore, in contrast to binding to VIM-2, in the L1 complex the Zn-bridging water is present and is stabilised by interaction with the rotated hydroxyethyl alcohol. By contrast with what has normally been reported for interactions of carbapenems with MBLs, the C-7 carboxylate does not interact with Zn1, but instead with Tyr32. Interactions of the faropenem-derived product with the L1 metal centre thus exclusively involve Zn2, which is ligated by the nitrogen and carboxylate of the thiazoline ring, as in the VIM-2 complexes. The C-7 carboxylate also forms hydrogen bonds with Ser221 (3.1 Å) and Ser223 (2.7 Å), residues previously reported to be involved in L1 binding to inhibitors and substrates [43,44].

The faropenem binding mode to L1 is similar to that observed for imipenem binding to the B3 MBL SMB-1 (PDB 5B1U), in which the hydrolysed carbapenem substrate is observed in the imine form (C-2 is sp^3 hybridized) and the C-7 carboxylate does not displace the Zn-bridging water (Figure S11). Further, in both structures, C-2 of the antibiotic-derived product is in the (*S*)-configuration. Comparison of the VIM-2:faropenem complex with the complex formed by reaction of meropenem with NDM-1[45], in which the deprotonated Δ^2-pyrroline (enamine) form was observed (C-2 is sp^2 hybridized) at 2.12 Å

resolution (Figure S12A), reveals similar binding modes in which the zinc bridging active site water is displaced. However, comparison with meropenem binding to VIM-1 shows differences in the positioning of the C-6 hydroxyethyl group that results in the presence of the zinc bridging active site water in the VIM-1:meropenem complex, but not in the VIM-2:faropenem complex (Figure S12B)[42].

2.3 Faropenem hydrolysis studied by NMR

We then investigated the relevance of the crystallographic observations to the β-lactamase-catalysed hydrolysis of faropenem in solution by using 1D and 2D NMR methods, initially with L1, KPC-2, and VIM-2 (Figure 6, S13-28). For comparison, we subsequently studied the reaction of faropenem with other SBLs/MBLs, i.e. the class D SBLs OXA-10, OXA-23 and OXA-48 and the B1 MBLs NDM-1 and VIM-1. Figures S13-28 show individual spectra; peaks were assigned based on the values in Table S2. The ^{1}H-NMR studies for KPC-2 (Figure S14), VIM-2 (Figure S16), L1 (Figure S13) and NDM-1 (Figure S15) were consistent with the prior kinetic analyses (Table 1), including with respect to KPC-2 manifesting the poorest rate of faropenem hydrolysis. In total, five faropenem-derived product structures were assigned, though low levels of other unassigned species were also observed (Figures 6, S13 and S15). Compounds **1** and **2** (major and minor, respectively) were observed in all cases and were assigned as the C-5 epimeric forms of the THF ring-closed enamines, with the (5*R*) minor product (**2**) arising from epimerisation of the major (5*S*) enamine (**1**). **1** is likely to be the major enzymatic product, consistent with studies on carbapenems [11,12]. The amounts of **1** and **2** decreased with time, due to their conversion to the imine-alkenes **3** and **4**, respectively, as confirmed by time-dependent analyses of evolution of faropenem-derived products on reaction with VIM-2 (Figure S28A).

Compounds **3** and **4** were observed in all cases and were assigned as (5*R*)-**3** and (5*S*)-**4** imines with an opened THF ring. The Z-alkene geometry was assigned on the basis of crystallographic analyses (see above) – it is likely but not certain that this is the alkene geometry in solution (Figures 6 and 7). **3** and **4** were observed to be formed from **1** and **2** non-enzymatically when using NMR to study the hydrolysis of faropenem alone, but at least in some cases may be direct enzyme products. The imine with a closed THF ring, **5,** was only observed with VIM-1 (minor product) and VIM-2 (a major product) (Figures 6, S16 and S17). NMR experiments following the time course of faropenem reaction with VIM-2 confirm this, with an initial increase in the amounts of compounds **1** and **2.** The presence of **1** and **2** decreases with time however, and there is a gradual increase of **3, 4** and **5** with time (Figure S28A).

The stereochemistry of **5** at C-2 was not assigned but is likely to be (2*S*), based upon our high-resolution crystallographic studies with L1 (Figures 4, 5 and S13). We did not obtain evidence for the C-5 epimer of **5**, i.e. **6** (Figure S8), though we cannot rule **6** out as a minor product. Note that C-5 epimerisation should be more facile for the enamines (**1**, **2**) than the imine tautomers (**3**-**6**). Thus, **5** is likely produced as direct result of VIM-1/VIM-2 catalysis; notably we saw no evidence for conversion of **1/2** to **5/6** (Figures 6 and 7).

Overall, the solution studies provide important information additional to the crystallographic observations (Figure 7). In the case of the L1 complex, the imine with the closed THF ring **5*** (*= crystallographically observed, Figure 7) was observed; however, **5** was not detected in the solution studies with L1 (Figures 6 and S13). It is possible that, in the case of L1, the crystallographically observed **5*** results from tautomerisation of L1 complexed enamine **1*** under the crystallographic analysis conditions. It is also possible that the crystallographically observed product **5*** is not released from the L1 active site in solution, though this seems less likely. Further, in the L1 crystal structures the C-2 configuration is clearly defined as (*S*), which could not be resolved by solution NMR. This observation contrasts with the recent crystal structure of a faropenem-derived product in OXA-48 in which the imine was modelled with C-2 in the (*R*)-configuration[46]. However, we note that the lower resolution of these OXA-48 crystallographic data [46], compared to L1 (2.10 Å vs 1.57 Å), makes assignment of the C-2 configuration in the OXA-48 structure uncertain. Although the same (2*S*)-**5*** product was modelled in crystal structure of the class A BlaC enzyme (PDB 4EBL), the electron density for the side chain in that case is poorly defined and inspection of the electron density is indicative of an sp^2 hybridized C-2 atom, ruling out the **5*** complex. In the KPC-2/VIM-2 crystal structures there was no evidence for formation of the imine with a closed THF ring (**5***); instead the THF ring-opened imine-alkene **3***, was modelled (Figures 6 and 7) and was observed in solution (**3**). However, whilst **3** could be produced as a direct enzyme product arising from **3***, the combined results indicate that it is more likely **3** that is at least predominantly produced from enamine **1** *via* **1*** (Figure 6); however it should be noted that in the case of VIM-1 **4** is a major product (Figures S17 and S28).

3 Discussion

From a chemical perspective, the penems are important in the history of β-lactams because, as hybrid penicillin-cephalosporin molecules, they were predicted to have improved properties as drugs. As yet, this has not been the case, at least in terms of major clinical impact. The penems are not natural products, unlike (as far as is known) the subsequently-identified naturally occurring but synthetically produced carbapenems that have undergone significant development to now include clinically-important antibacterials[12]. The reasons for the relative lack of development of the penems are unclear; they may reflect difficulties in synthesis (these should be surmountable), stability (this should also be surmountable), and/or toxicity. Despite these potential issues, given that faropenem is orally active and all carbapenems are injected medicines (carbapenem prodrugs are reported), it would seem more research on penems is merited. Only one penem has been approved for clinical use, i.e., faropenem, the subject of our study.

Our results, together with those previously reported[10,13], further highlight the potential of penems as β-lactamase inhibitors. They imply that, once faropenem has reacted with the β-lactamase, the acyl-enzyme (SBL) or analogous Zn(II) complexed intermediate (MBL) can undergo various fates depending on the precise nature of the active site. One possibility is protonation of the β-lactam derived nitrogen followed by release of a hydrolysed enamine (**1**, Figures 6 and 7), in a manner analogous to that proposed for the release of hydrolysed carbapenems[47]. Alternatively, at least in the case of some, but not all, MBLs (VIM-1 and

VIM-2, but not L1 or NDM-1 in our studies), the enamine can tautomerise with protonation at C-2 to give an imine product with a closed THF ring (**5**). The nascent product (**1**) can epimerise at C-5 to give **2**; **1** and **2** can also rearrange to give imines with the THF ring opened (**3**,**4**), though in some cases we cannot rule out that **3** and/or **4** are direct enzyme products (Figures S17 and S28B). The results also show that subtle differences between active sites can alter reaction outcomes and kinetics, and that static crystallographic studies do not necessarily reflect solution observations, hence inhibition profiles. Further experiments should be done to see if any of these compounds display inhibitory properties against MBLs and/or SBLs.

Previous studies have also shown that when reacted with nucleophilic cysteine enzymes, e.g. the LdtMT2 transpeptidase from *M. tuberculosis*, faropenem can react to give a thioester linked complex that can undergo C-5-C-6 fragmentation[14,47]. Other modes of penem reactivity can also be envisaged, for example by the conjugate addition to the alkene in the intact penem. An alternative mode of penem reactivity is manifested by C-6 exomethylene penems such as BRL-42715, a potent inhibitor of some SBLs, which reacts to give an acyl-enzyme complex that converts to an aminoacrylate[19,20].

The combined results presented here and previously thus demonstrate that initially formed enzyme-penem complexes can have many potential fates – a property that might be useful in identifying a single compound that potently inhibits multiple different classes of enzymes (e.g. SBLs/MBLs/transpeptidases), by reacting in multiple ways to give stable enzyme-inhibitor complexes. Such an ability is manifest in certain other β-lactam containing β-lactamase inhibitors, e.g. some clavams / oxapenems[19,20]. Although other classes of non β-lactam containing β-lactam inhibitors might have this potential, very few (if any) have the demonstrated clinical utility of bicyclic β-lactams. We thus suggest there is considerable reason for renewed efforts to synthesise new penems and related β-lactam containing compounds for testing as β-lactamase inhibitors and antibiotics. Drug discovery efforts on penems and related compounds should perhaps involve extensive synthetic efforts combined with screening against multiple clinically relevant bacteria and enzyme targets, and rigorous characterisation of the resulting products and inhibitory species, in order to investigate the full potential of compounds that can react *via* alternative reaction pathways.

Supplementary Material

Refer to Web version on PubMed Central for supplementary material.

Acknowledgments

We thank the Medical Research Council MRC (MR/T016035/1), EPSRC, National Institute of Allergy and Infectious Diseases of the National Institutes of Health (NIH, R01AI100560 to J.S.) and Wellcome Trust for funding our research and Diamond Light Source and their beamline scientists for aiding with data collection. TRM is funded by the BBSRC (BB/M011224/1). PR thanks the Deutsche Akademie für Naturforscher Leopoldina, Germany, for funding a postdoctoral fellowship. The content is solely the responsibility of the authors and does not necessarily represent the official views of the NIH.

References

[1]. Fair RJ, Tor Y. Antibiotics and Bacterial Resistance in the 21st Century. Perspect Medicin Chem. 2014; 6 doi: 10.4137/PMC.S14459

[2]. Bush K, Jacoby GA. Updated functional classification of beta-lactamases. Antimicrob Agents Chemother. 2010; 54: 969–76. DOI: 10.1128/AAC.01009-09 [PubMed: 19995920]

[3]. Bush K. Metallo-beta-lactamases: a class apart. Clin Infect Dis. 1998; 27 (Suppl 1) S48–53. accessed May 29, 2018 [PubMed: 9710671]

[4]. Bebrone C. Metallo-β-lactamases (classification, activity, genetic organization, structure, zinc coordination) and their superfamily. Biochem Pharmacol. 2007; 74: 1686–1701. DOI: 10.1016/j.bcp.2007.05.021 [PubMed: 17597585]

[5]. Lisa M-N, Palacios AR, Aitha M, González MM, Moreno DM, Crowder MW, Bonomo RA, Spencer J, Tierney DL, Llarrull LI, Vila AJ. A general reaction mechanism for carbapenem hydrolysis by mononuclear and binuclear metallo-β-lactamases. Nat Commun. 2017; 8: 538. doi: 10.1038/s41467-017-00601-9 [PubMed: 28912448]

[6]. Tooke CL, Hinchliffe P, Bragginton EC, Colenso CK, Hirvonen VHA, Takebayashi Y. β-Lactamases and β-Lactamase Inhibitors in the 21st Century. J Mol Biol. 2019; 431: 3472–3500. DOI: 10.1016/J.JMB.2019.04.002 [PubMed: 30959050]

[7]. Bush K, Bradford PA. β-Lactams and β-Lactamase Inhibitors: An Overview. Cold Spring Harb Perspect Med. 2016; 6 doi: 10.1101/cshperspect.a025247

[8]. Leavitt A, Navon-Venezia S, Chmelnitsky I, Schwaber MJ, Carmeli Y. Emergence of KPC-2 and KPC-3 in Carbapenem-Resistant Klebsiella pneumoniae Strains in an Israeli Hospital. Antimicrob Agents Chemother. 2007; 51: 3026–3029. DOI: 10.1128/AAC.00299-07 [PubMed: 17562800]

[9]. Shen P, Wei Z, Jiang Y, Du X, Ji S, Yu Y, Li L. Novel genetic environment of the carbapenem-hydrolyzing beta-lactamase KPC-2 among Enterobacteriaceae in China. Antimicrob Agents Chemother. 2009; 53: 4333–8. DOI: 10.1128/AAC.00260-09 [PubMed: 19620332]

[10]. Lohans CT, van Groesen E, Kumar K, Tooke CL, Spencer J, Paton RS, Brem J, Schofield CJ. A New Mechanism for β-Lactamases: Class D Enzymes Degrade 1β-Methyl Carbapenems through Lactone Formation. Angew Chemie Int. 2018; 57: 1282–1285. DOI: 10.1002/anie.201711308

[11]. Walsh TR, Toleman MA, Poirel L, Nordmann P. Metallo-beta-lactamases: the quiet before the storm? Clin Microbiol Rev. 2005; 18: 306–25. DOI: 10.1128/CMR.18.2.306-325.2005 [PubMed: 15831827]

[12]. Papp-Wallace KM, Endimiani A, Taracila MA, Bonomo RA. Carbapenems: Past, Present, and Future. Antimicrob Agents Chemother. 2011; 55: 4943. doi: 10.1128/AAC.00296-11 [PubMed: 21859938]

[13]. van Groesen E, Lohans CT, Brem J, Aertker KM, Claridge TD, Schofield C. 19F-NMR Monitoring of Reversible Protein Post-Translational Modifications: Class D β-Lactamase Carbamylation and Inhibition. Chem – A Eur J. 2019; doi: 10.1002/chem.201902529

[14]. Lohans CT, Chan HTH, Malla TR, Kumar K, Kamps JJAG, McArdle DJB, van Groesen E, de Munnik M, Tooke CL, Spencer J, Paton RS, et al. Non-Hydrolytic β-Lactam Antibiotic Fragmentation by l,d -Transpeptidases and Serine β-Lactamase Cysteine Variants. Angew Chemie Int. 2019; 58: 1990–1994. DOI: 10.1002/anie.201809424

[15]. Dalhoff A, Janjic N, Echols R. Redefining penems. Biochem Pharmacol. 2006; 71: 1085–1095. DOI: 10.1016/J.BCP.2005.12.003 [PubMed: 16413506]

[16]. Ernest I, Gosteli J, Greengrass CW, Holick W, Pfaendler HR, Woodward RB. The penems, a new class of .beta.-lactam antibiotics: 6-acylaminopenem-3-carboxylic acids. J Am Chem Soc. 1978; 100: 8214–8222. DOI: 10.1021/ja00494a032

[17]. Hamilton-Miller JMT. Chemical and Microbiologic Aspects of Penems, a Distinct Class of β-Lactams: Focus on Faropenem. Pharmacotherapy. 2003; 23: 1497–1507. DOI: 10.1592/phco.23.14.1497.31937 [PubMed: 14620395]

[18]. Okamoto K, Gotoh N, Nishino T. Pseudomonas aeruginosa reveals high intrinsic resistance to penem antibiotics: penem resistance mechanisms and their interplay. Antimicrob Agents Chemother. 2001; 45: 1964–71. DOI: 10.1128/AAC.45.7.1964-1971.2001 [PubMed: 11408209]

[19]. Michaux, Catherine; Charlier, Paulette; Frère, Jean-Marie; Wouters, Johan. Crystal Structure of BRL 42715, C6-(N1-Methyl-1,2,3-triazolylmethylene)penem. Complex with Enterobacter cloacae 908R β-Lactamase: Evidence for a Stereoselective Mechanism from Docking Studies. 2005; doi: 10.1021/JA0426241

[20]. Coleman K, Griffin DR, Page JW, Upshon PA. In vitro evaluation of BRL 42715, a novel beta-lactamase inhibitor. Antimicrob Agents Chemother. 1989; 33: 1580–7. DOI: 10.1128/aac.33.9.1580 [PubMed: 2817854]

[21]. Qu X, Yin C, Sun X, Huang S, Li C, Dong P, Lu X, Zhang Z, Yin A. Consumption of antibiotics in Chinese public general tertiary hospitals (2011-2014): Trends, pattern changes and regional differences. PLoS One. 2018; 13 doi: 10.1371/JOURNAL.PONE.0196668

[22]. Gandra S, Klein EY, Pant S, Malhotra-Kumar S, Laxminarayan R. Faropenem Consumption is Increasing in India. Clin Infect Dis. 2016; 62: 1050.2–1052. DOI: 10.1093/cid/ciw055

[23]. Karlowsky JA, Adam HJ, Baxter MR, Denisuik AJ, Lagacé-Wiens PRS, Walkty AJ, Puttagunta S, Dunne MW, Zhanel GG. In Vitro Activity of Sulopenem, an Oral Penem, against Urinary Isolates of Escherichia coli. Antimicrob Agents Chemother. 2019; 63 doi: 10.1128/AAC.01832-18

[24]. Dhar N, Dubée V, Ballell L, Cuinet G, Hugonnet J-E, Signorino-Gelo F, Barros D, Arthur M, McKinney JD. Rapid cytolysis of Mycobacterium tuberculosis by faropenem, an orally bioavailable β-lactam antibiotic. Antimicrob Agents Chemother. 2015; 59: 1308–19. DOI: 10.1128/AAC.03461-14 [PubMed: 25421469]

[25]. Schneider I, Queenan AM, Markovska R, Markova B, Keuleyan E, Bauernfeind A. New variant of CTX-M-type extended-spectrum beta-lactamases, CTX-M-71, with a Gly238Cys substitution in a Klebsiella pneumoniae isolate from Bulgaria. Antimicrob Agents Chemother. 2009; 53: 4518–21. DOI: 10.1128/AAC.00461-09 [PubMed: 19620330]

[26]. Lu Z, Wang H, Zhang A, Liu X, Zhou W, Yang C, Guddat L, Yang H, Schofield CJ, Rao Z. Structures of Mycobacterium tuberculosis Penicillin-Binding Protein 3 in Complex with Five β-Lactam Antibiotics Reveal Mechanism of Inactivation. Mol Pharmacol. 2020; 97: 287–294. DOI: 10.1124/mol.119.118042 [PubMed: 32086254]

[27]. EM S, G S, R S. Binding and processing of β-lactam antibiotics by the transpeptidase Ldt Mt2 from Mycobacterium tuberculosis. FEBS J. 2017; 284 doi: 10.1111/FEBS.14010

[28]. P OA, Z X, C Y. Molecular Basis of Substrate Recognition and Product Release by the Klebsiella Pneumoniae Carbapenemase (KPC-2). J Med Chem. 2017; 60 doi: 10.1021/ACS.JMEDCHEM.7B00158

[29]. Aitha M, Marts AR, Bergstrom A, Møller AJ, Moritz L, Turner L, Nix JC, Bonomo RA, Page RC, Tierney DL, Crowder MW. Biochemical, mechanistic, and spectroscopic characterization of metallo-β-lactamase VIM-2. Biochemistry. 2014; 53: 7321–31. DOI: 10.1021/bi500916y [PubMed: 25356958]

[30]. Spencer J, Clarke AR, Walsh TR. Novel Mechanism of Hydrolysis of Therapeutic β-Lactams by Stenotrophomonas maltophilia L1 Metallo-β-lactamase. J Biol Chem. 2001; doi: 10.1074/jbc.M105550200

[31]. Kim Y, Tesar C, Mire J, Jedrzejczak R, Binkowski A, Babnigg G, Sacchettini J, Joachimiak A. Structure of apo- and monometalated forms of NDM-1--a highly potent carbapenem-hydrolyzing metallo-β-lactamase. PLoS One. 2011; 6 e24621 doi: 10.1371/journal.pone.0024621 [PubMed: 21931780]

[32]. Stoczko M, Frère J-M, Rossolini GM, Docquier J-D. Postgenomic scan of metallo-beta-lactamase homologues in rhizobacteria: identification and characterization of BJP-1, a subclass B3 ortholog from Bradyrhizobium japonicum. Antimicrob Agents Chemother. 2006; 50: 1973–81. DOI: 10.1128/AAC.01551-05 [PubMed: 16723554]

[33]. Tooke CL, Hinchliffe P, Bonomo RA, Schofield CJ, Mulholland AJ, Spencer J. Natural variants modify Klebsiella pneumoniae carbapenemase (KPC) acyl-enzyme conformational dynamics to extend antibiotic resistance. J Biol Chem. 2020; doi: 10.1074/JBC.RA120.016461

[34]. Tooke CL, Hinchliffe P, Lang PA, Mulholland AJ, Brem J, Schofield CJ, Spencer J. Molecular Basis of Class A β-Lactamase Inhibition by Relebactam. Antimicrob Agents Chemother. 2019; 63 doi: 10.1128/AAC.00564-19

[35]. Ullah JH, Walsh TR, Taylor IA, Emery DC, Verma CS, Gamblin SJ, Spencer J. The crystal structure of the L1 metallo-β-lactamase from Stenotrophomonas maltophilia at 1.7 å resolution 1. Nagai K. J Mol Biol. 1998; 284: 125–136. DOI: 10.1006/jmbi.1998.2148 [PubMed: 9811546]

[36]. Pemberton OA, Zhang X, Chen Y. Molecular Basis of Substrate Recognition and Product Release by the Klebsiella pneumoniae Carbapenemase (KPC-2). J Med Chem. 2017; 60: 3525–3530. DOI: 10.1021/acs.jmedchem.7b00158 [PubMed: 28388065]

[37]. Fonseca F, Chudyk EI, Van Der Kamp MW, Correia A, Mulholland AJ, Spencer J. The basis for carbapenem hydrolysis by class a β-lactamases: A combined investigation using crystallography and simulations. J Am Chem Soc. 2012; 134: 18275–18285. DOI: 10.1021/ja304460j [PubMed: 23030300]

[38]. Fisher, Jed F; Meroueh, Samy O; Mobashery, S. Bacterial Resistance to β-Lactam Antibiotics: Compelling Opportunism. Compelling Opportunity. 2005; doi: 10.1021/CR030102I

[39]. Brem J, Cain R, Cahill S, McDonough MA, Clifton IJ, Jiménez-Castellanos J-C, Avison MB, Spencer J, Fishwick CWG, Schofield CJ. Structural basis of metallo-β-lactamase, serine-β-lactamase and penicillin-binding protein inhibition by cyclic boronates. Nat Commun. 2016; 7 12406 doi: 10.1038/ncomms12406 [PubMed: 27499424]

[40]. Hinchliffe P, González MM, Mojica MF, González JM, Castillo V, Saiz C, Kosmopoulou M, Tooke CL, Llarrull LI, Mahler G, Bonomo RA, et al. Cross-class metallo-β-lactamase inhibition by bisthiazolidines reveals multiple binding modes. Proc Natl Acad Sci U S A. 2016; 113: E3745–E3754. DOI: 10.1073/pnas.1601368113 [PubMed: 27303030]

[41]. Hinchliffe P, Tanner CA, Krismanich AP, Labbé G, Goodfellow VJ, Marrone L, Desoky AY, Calvopiña K, Whittle EE, Zeng F, Avison MB, et al. Structural and Kinetic Studies of the Potent Inhibition of Metallo-β-lactamases by 6-Phosphonomethylpyridine-2-carboxylates. Biochemistry. 2018; 57: 1880–1892. DOI: 10.1021/acs.biochem.7b01299 [PubMed: 29485857]

[42]. Salimraj R, Hinchliffe P, Kosmopoulou M, Tyrrell JM, Brem J, van Berkel SS, Verma A, Owens RJ, McDonough MA, Walsh TR, Schofield CJ, et al. Crystal structures of VIM-1 complexes explain active site heterogeneity in VIM-class metallo-β-lactamases. FEBS J. 2019; 286: 169–183. DOI: 10.1111/febs.14695 [PubMed: 30430727]

[43]. Hinchliffe P, González MM, Mojica MF, González JM, Castillo V, Saiz C, Kosmopoulou M, Tooke CL, Llarrull LI, Mahler G, Bonomo RA, et al. Cross-class metallo-β-lactamase inhibition by bisthiazolidines reveals multiple binding modes. Proc Natl Acad Sci. 2016; 113: E3745–E3754. DOI: 10.1073/PNAS.1601368113 [PubMed: 27303030]

[44]. Spencer J, Read J, Sessions RB, Howell S, Blackburn GM, Gamblin SJ. Antibiotic recognition by binuclear metallo-beta-lactamases revealed by X-ray crystallography. J Am Chem Soc. 2005; 127: 14439–44. DOI: 10.1021/ja0536062 [PubMed: 16218639]

[45]. King DT, Worrall LJ, Gruninger R, Strynadka NCJ. New Delhi metallo-β-lactamase: structural insights into β-lactam recognition and inhibition. J Am Chem Soc. 2012; 134: 11362–5. DOI: 10.1021/ja303579d [PubMed: 22713171]

[46]. Akhtar A, Pemberton OA, Chen Y. Structural Basis for Substrate Specificity and Carbapenemase Activity of OXA-48 Class D β-Lactamase. ACS Infect Dis. 2020; 6: 261–271. DOI: 10.1021/acsinfecdis.9b00304 [PubMed: 31872762]

[47]. Lohans CT, Freeman EI, van Groesen E, Tooke CL, Hinchliffe P, Spencer J, Brem J, Schofield CJ. Mechanistic Insights into β-Lactamase-Catalysed Carbapenem Degradation Through Product Characterisation. Sci Rep. 2019; 9 13608 doi: 10.1038/s41598-019-49264-0 [PubMed: 31541180]

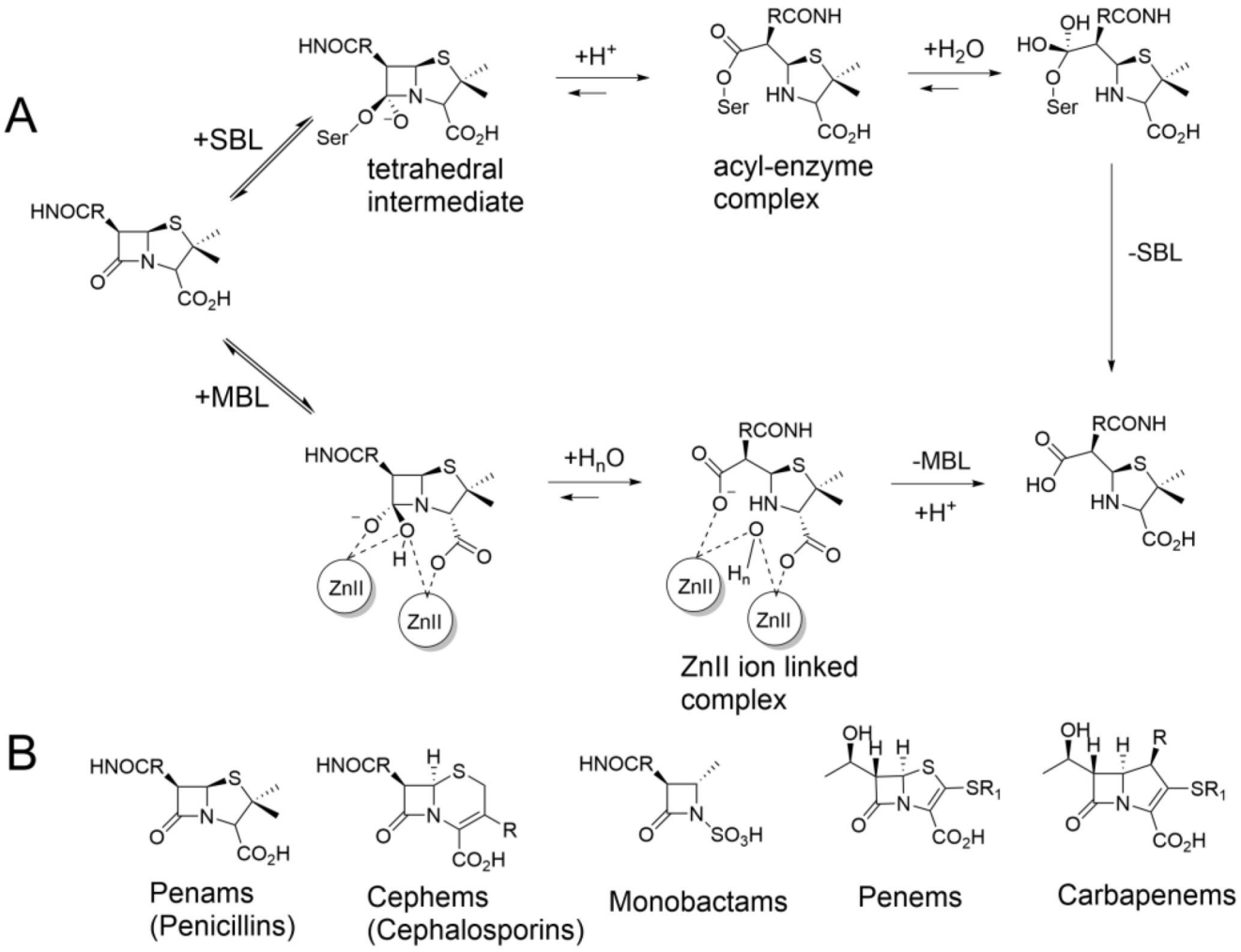

Figure 1. β-Lactam hydrolysis by serine and metallo-β-lactamase.

(A) SBL catalysis proceeds via an acyl-enzyme complex formed after being hydrolysed via a transient tetrahedral intermediate. In MBL catalysis, a zinc ion activated water molecule (that bridges the two Zn ions in the resting states of B1 and B3 MBLs), reacts with the β-lactam ring. Hydrolysis also proceeds via a transient tetrahedral intermediate and a hydrolysed intermediate stabilised through interactions with the Zn ions[6]. (B) Classes of clinically used β-lactam antibiotics.

Europe PMC Funders Author Manuscripts

Europe PMC Funders Author Manuscripts

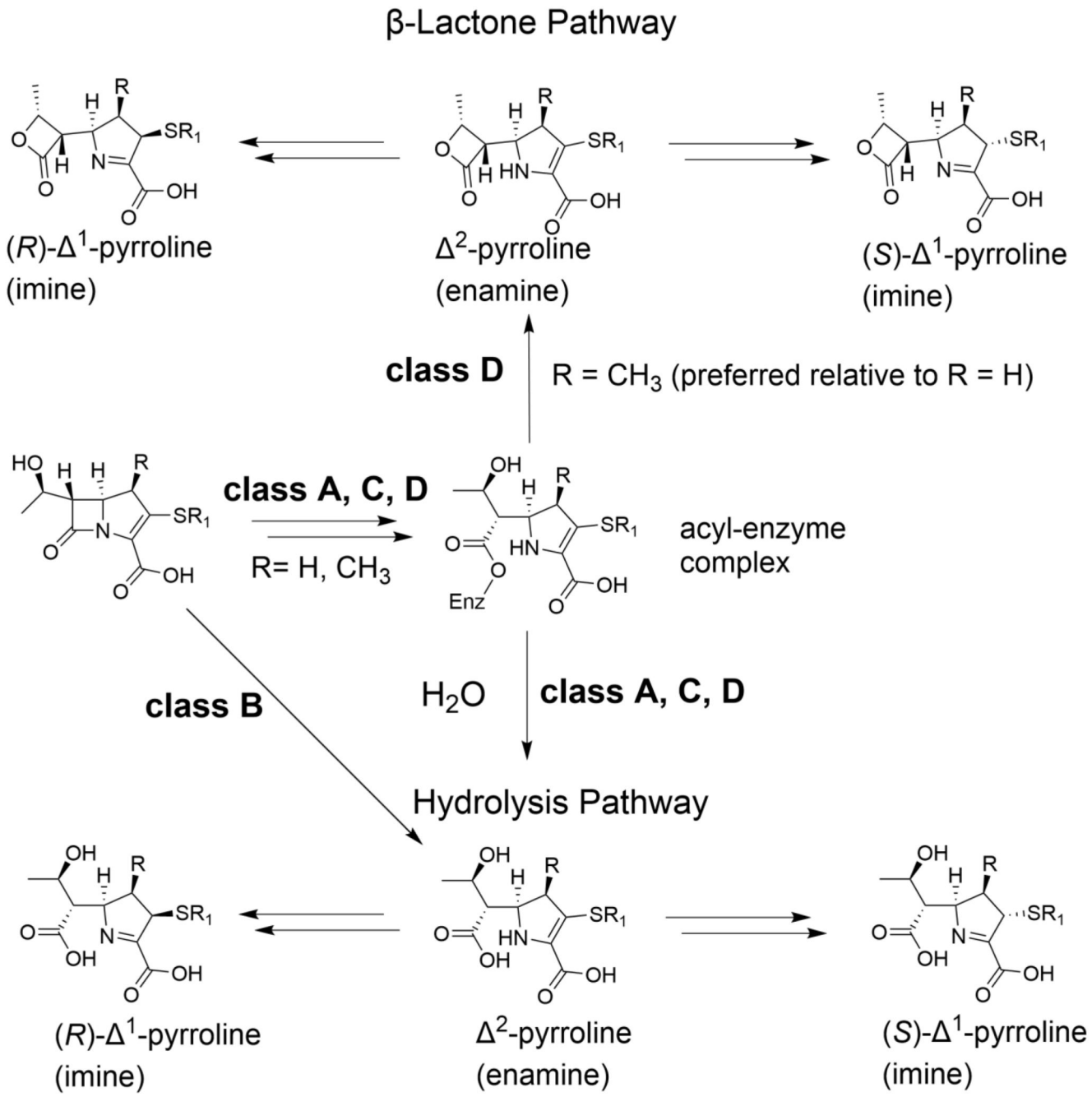

Figure 2. Carbapenem hydrolysis by β-lactamases.

SBL and MBL catalysed carbapenem hydrolysis is proposed to result (predominantly) in the initial formation of an enamine (Δ^2-pyrroline) that isomerises to give [(2*R*)- and (2*S*)-Δ^1-imine] products[10,13]. Various isomeric imine / enamine forms of reacted carbapenems have been observed crystallographically at transpeptidase/SBL/MBL active sites. In the case of the class D SBLs, the acyl-enzyme intermediate can also react to give lactone products.

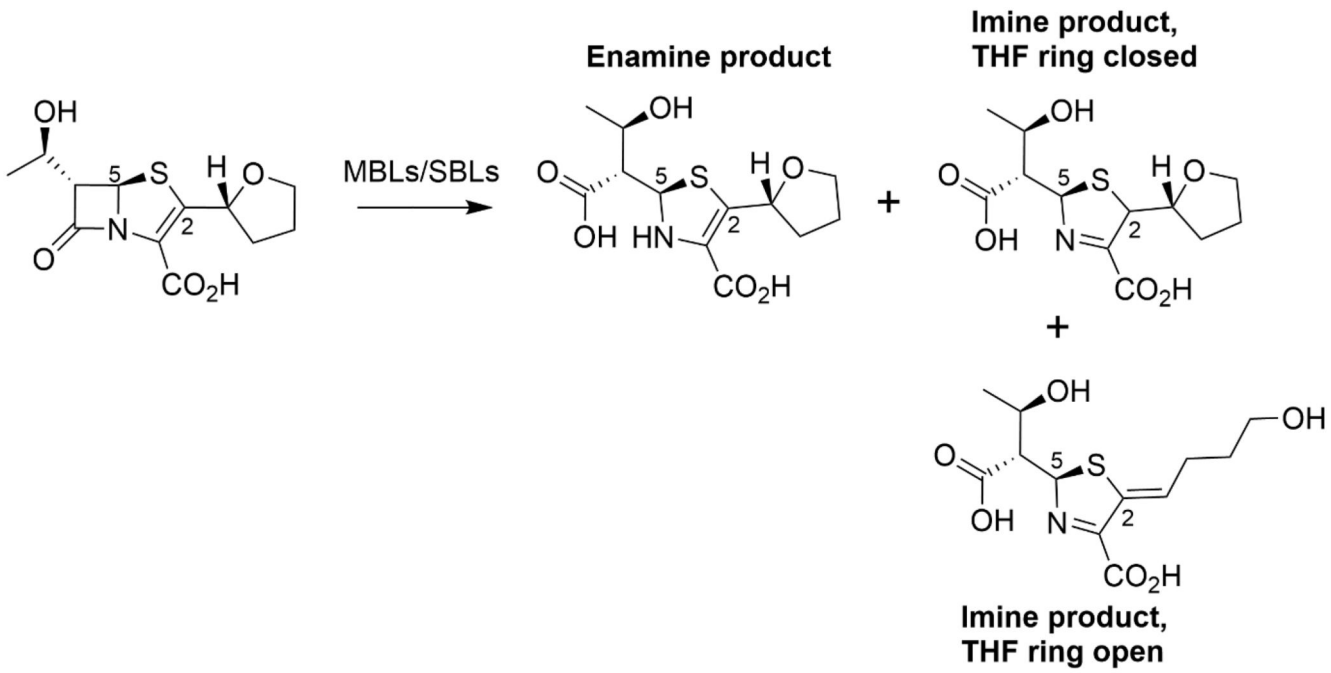

Figure 3. Potential reaction products of β-lactamase catalysed faropenem hydrolysis.
Note the possibility of isomer formation, e.g. epimerisation at C-5.

Europe PMC Funders Author Manuscripts

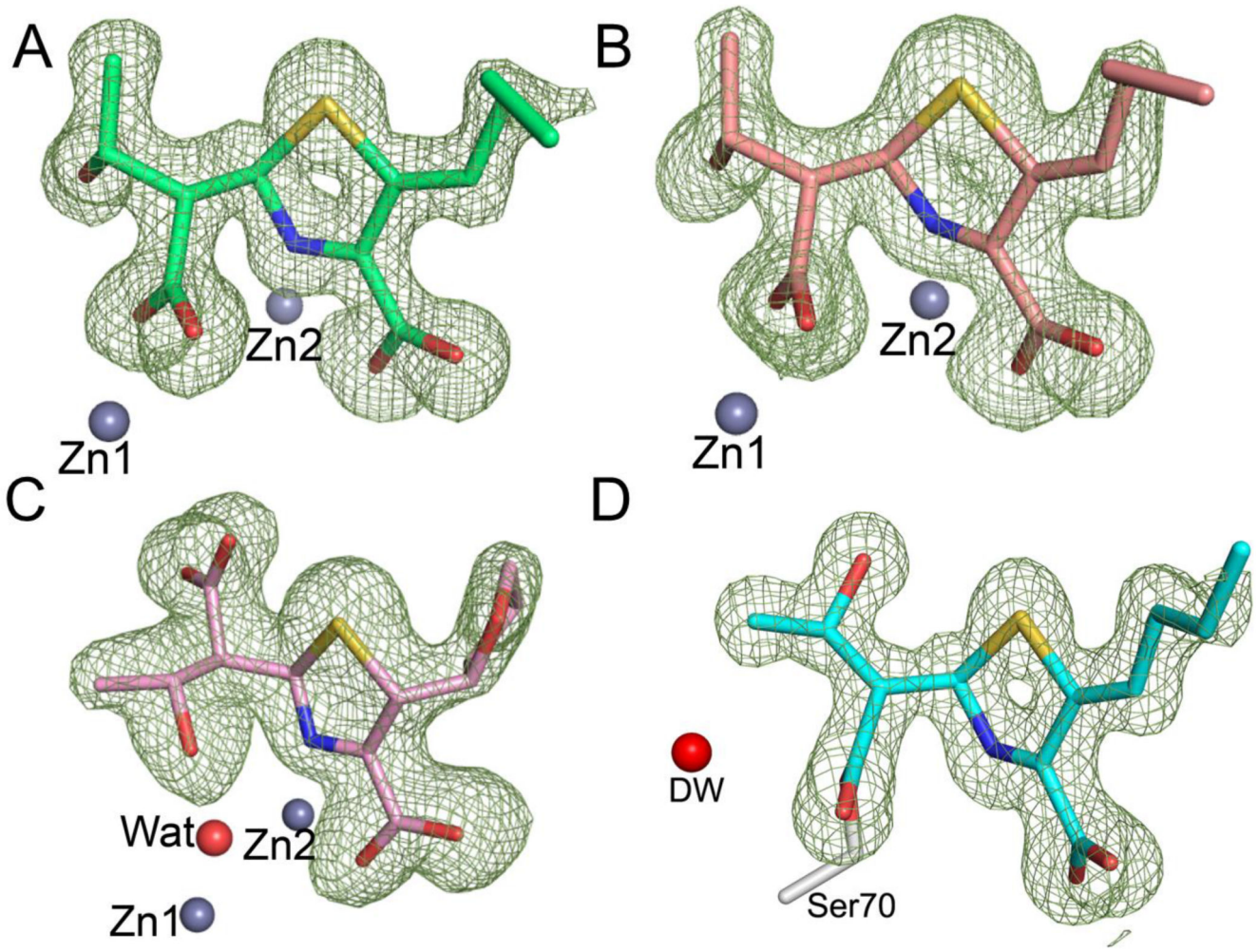

Figure 4. Faropenem derived complexes in the β-lactamase active sites as defined by electron density maps.

Views from the β-lactamase active sites, with the F_o-F_c electron density (green mesh, contoured at 3σ) calculated from the final model after removal of the ligand. (A) VIM-2, in the *I*222 space group (green, PDB code 7A5Z). (B) VIM-2 in the *C*2 space group (light red, PDB code 7A60). (C) L1 (pink, PDB code 7A63) and (D) KPC-2 (cyan, PDB code 7A61). The deacylating water (DW) is shown as a red sphere. Note the different conformations of the β-lactam derived carboxylate and hydroxyethyl groups in L1 compared to VIM-2 and the presence of the zinc bridging water with L1 (Wat, red sphere), but not VIM-2. No density was observed for the hydroxyl of the fragmented THF ring so it was omitted from the final models of the VIM-2 and KPC-2 complexes.

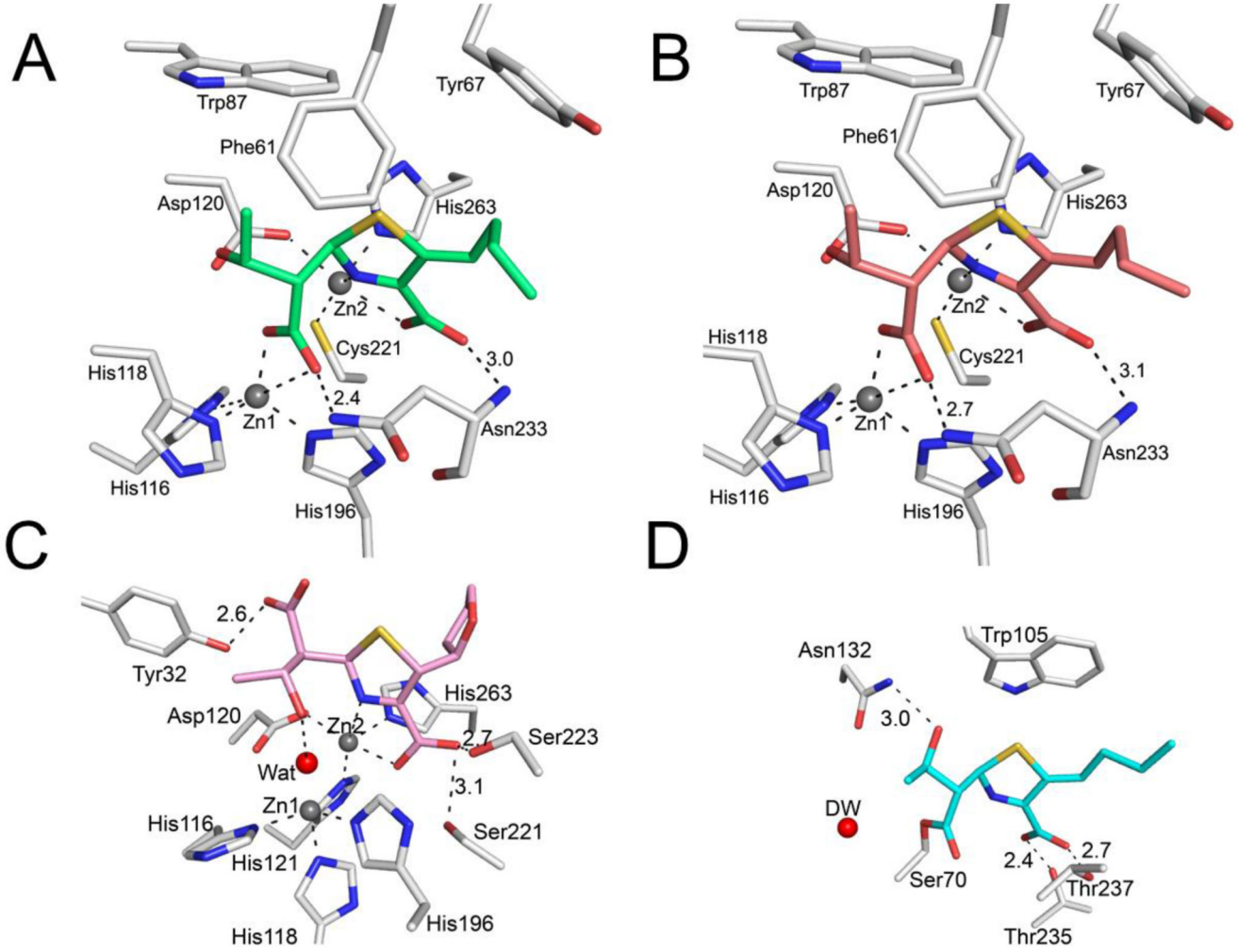

Figure 5. Interactions of the faropenem-derived complexes with serine- and metallo-β-lactamase active sites.

Protein residues are in light grey; faropenem-derived atoms are coloured as in Figure 4. Zinc ions are shown as grey spheres and the catalytic water (Wat) as a red sphere. Metal coordination and hydrogen bonds are shown as black dashes, with the distances labelled in Å. (A) VIM-2 (*I*222 space group), PDB 7A5Z; (B) VIM-2 (*C*2 space group) PDB 7A60; (C) L1 PDB 7A63; (D) KPC-2 PDB 7A61. Note the different conformations of the hydroxyethyl group in L1 (C) compared to VIM-2, leading to a lack of interaction with Zn1. KPC-2 (D) forms an acyl-enzyme complex with the faropenem derived complex.

Europe PMC Funders Author Manuscripts

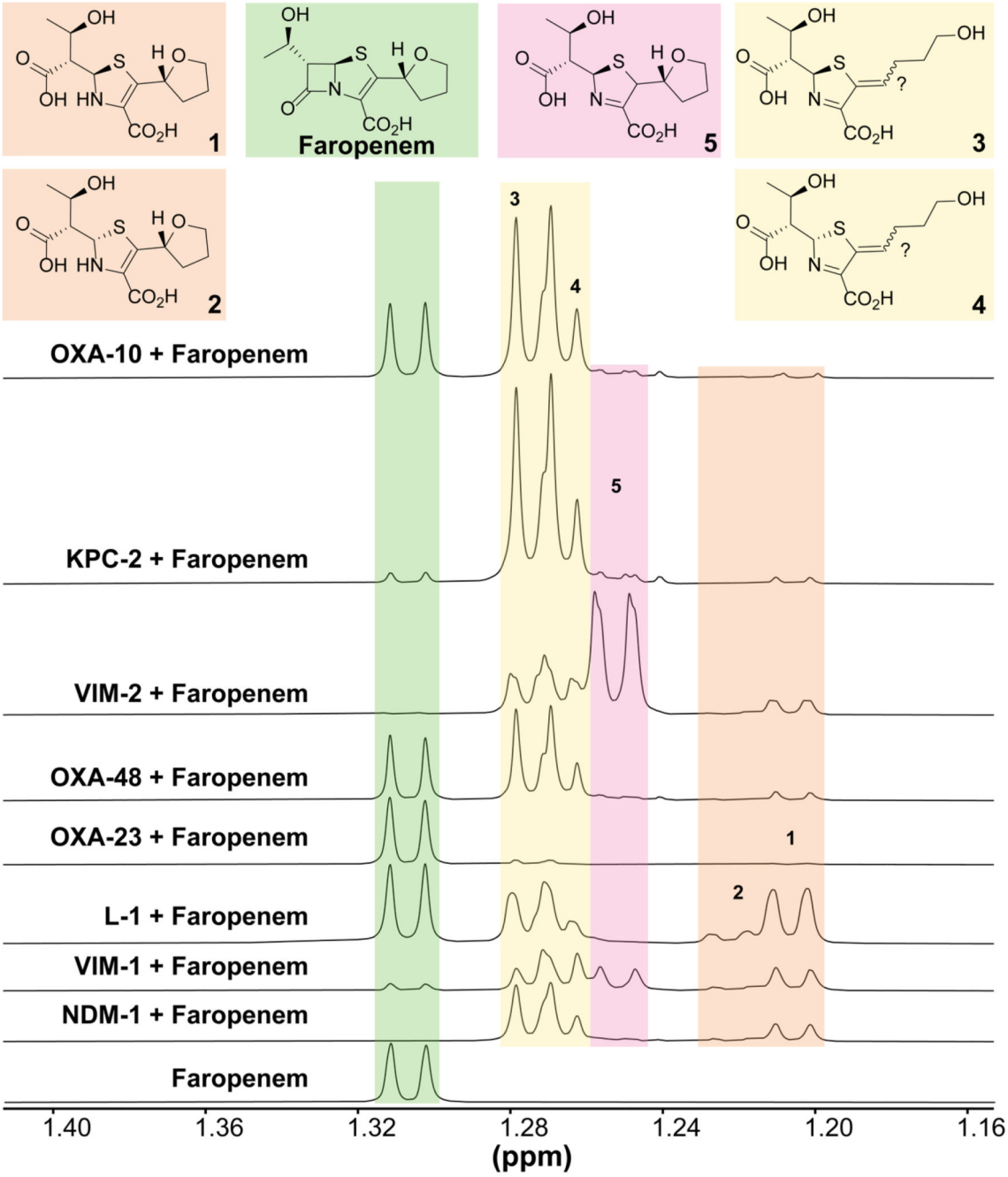

Figure 6. ^{1}H NMR (AVIII 700 MHz) spectra displaying methyl group resonances of the faropenem derived products.

Enamines **1** and **2** ((5*S*) and (5*R*) enamine THF ring-closed products, orange), THF ring-opened (5*R*) and (5*S*) imines **3** and **4** (yellow) and THF ring closed imine **5** (pink) degradation products were formed after incubation of faropenem (green) with OXA-10 (5 μM, 16 h), OXA-23 (5 μM, 15 min), OXA-48 (5 μM, 55 min), VIM-1 (280 nM, 5 min), VIM-2 (280 nM, 5 min), NDM-1 (5 μM, 5 min), KPC-2 (125 nM, 72 min), L1 (125 nM, 5 min). All enzymes were incubated with 5 mM faropenem apart from OXA-23, which was

incubated with 2 mM faropenem. Reactions were in 50 mM sodium phosphate, pH 7.5, 10% (*v/v*) D_2O. Note, **5** is only observed with VIM-1 and VIM-2. Colour coding corresponds to the structures shown and associated resonances. Individual spectra are provided in Figures S13-19. Characterisation data for compounds **2** and **5** are available in Figure 21 and Figures S22-27 respectively.

Europe PMC Funders Author Manuscripts

Europe PMC Funders Author Manuscripts

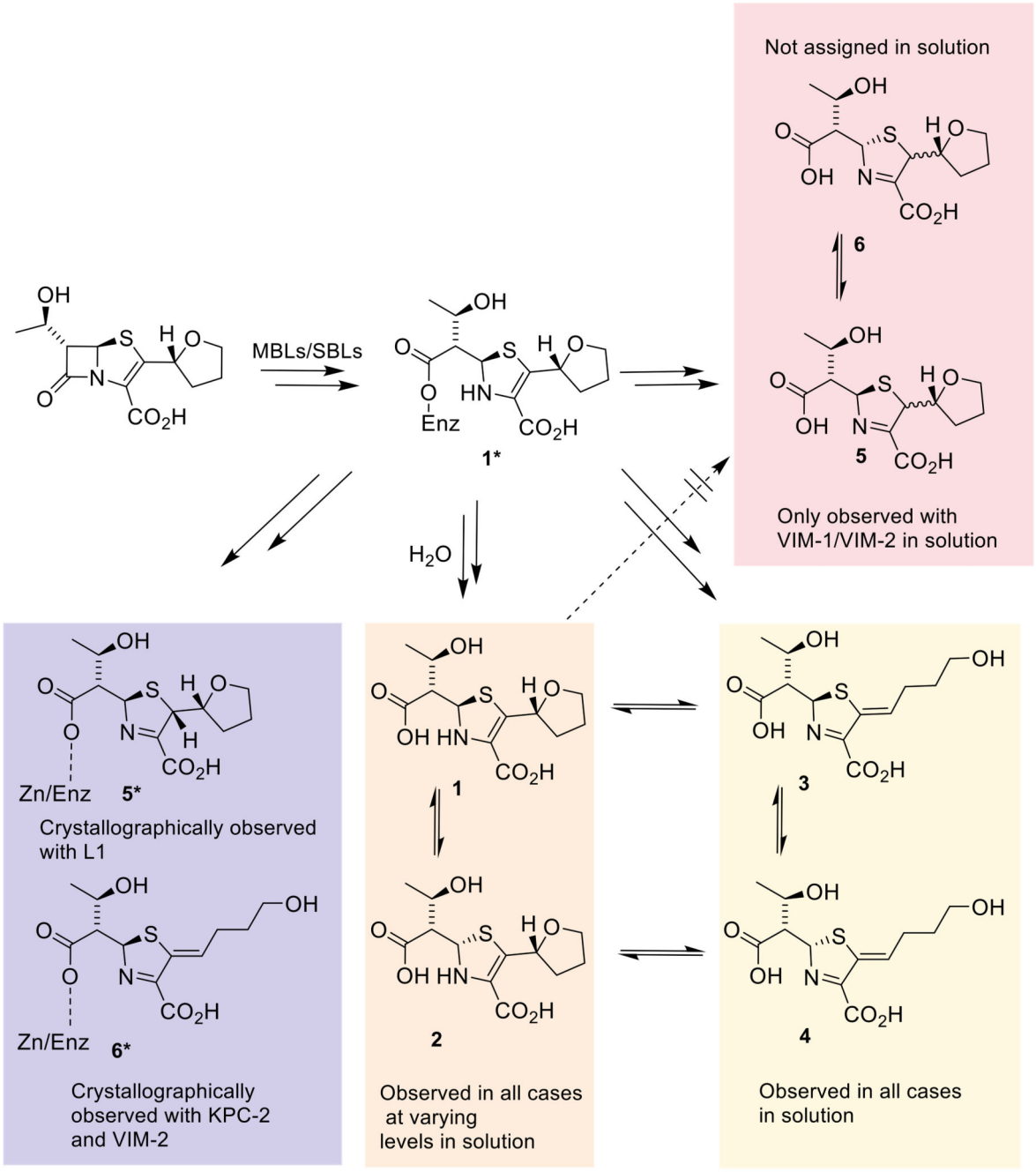

Figure 7. Summary of solution and crystallographic observations for faropenem reactions with SBLs/MBLs.

*Denotes crystallographically observed enzyme bound complexes. Note that **5** and **6** were only observed in the cases of solution studies with VIM-1 and VIM-2.

Europe PMC Funders Author Manuscripts

Table 1

Steady state kinetic parameters for faropenem turnover including reported values.

Enzyme	Type	Class	k_{cat} (s^{-1})	K_M (μM)	k_{cat}/K_M (s^{-1} $μM^{-1}$)	K_i (μM)
KPC-2	SBL	A	3.71 (0.21)	16.6 (3.84)	0.22	44.1 (25.0)
VIM-2	MBL	B1	36.7 (1.03)	5.11 (0.63)	7.17	-
L1	MBL	B3	43.7 (2.70)	36.3 (8.80)	1.20	-
BlaC[24]	SBL	A	0.91 (0.03)	23 (3)	0.040	-
NDM-1[31]	MBL	B1	14.7 (0.08)	99 (0.16)	0.15	-
BJP-1[32]	MBL	B3	2 (<0.2)	245 (<25)	0.008	-

Standard errors of the mean in parenthesis (n=3). See Experimental Section for KPC-2, VIM-2 and L1 assay details.